RASĀYAN *J. Chem.*
Vol. 15 | No. 4 |2866-2872| October - December | 2022
ISSN: 0974-1496 | e-ISSN: 0976-0083 | CODEN: RJCABP
http://www.rasayanjournal.com
http://www.rasayanjournal.co.in

APPLICATION OF PHOTOSENSITIZER-INCORPORATED INDIUM OXIDE NANOPARTICLES IN PHOTODYNAMIC THERAPY

Indrajit Roy[1], Raju Tiwari[1], Mahendra Nath[1], Surinder P Singh[2], Surendra Kumar[3], Darshan Singh[4] and Anuradha[4,] ✉

[1]Department of Chemistry, University of Delhi, Delhi-110007, India. Email:
[2]National Physical Laboratory, Dr. K. S. Krishnan Marg, New Delhi-110012, India.
[3]Department of Chemistry, Hansraj College, University of Delhi, Delhi -110007
[4]Department of Chemistry, Daulat Ram College, University of Delhi, Delhi -110007
✉Corresponding Author: anuradhabhardwaj30@gmail.com

ABSTRACT

Many disorders, both cancerous and non-cancerous, may be effectively treated using photodynamic therapy. In this scenario, photosensitizer drugs are first excited by light of the appropriate wavelength (in the visible-NIR range), after which they transmit their extra energy to molecular oxygen, resulting in the creation of strongly cytotoxic singlet oxygen. Indium oxide nanoparticles are optically transparent materials and can be used to incorporate fluorophores and photosensitizer drugs. Herein, we report the use of indium oxide nanoparticles incorporated with a photosensitizer. These nanoparticles have been synthesized in a methanolic medium. The characterization of prepared nanoparticles included FTIR, XRD, TEM, and optical studies (UV-visible and fluorescence spectroscopy). Cell viability studies demonstrated that the photosensitizer-incorporated nanoparticles showed cytotoxic effects only upon light irradiation. The results indicate the promise of photosensitizer-incorporated indium oxide nanoparticles as delivery agents in photodynamic therapy.

Keywords: Photodynamic Therapy (PDT), Photosensitizer (PS), Laser Light, Singlet Oxygen ($^1O_2$), Cytotoxicity.
RASĀYAN *J. Chem.*, Vol. 15, No. 4, 2022

INTRODUCTION

A large band-gap, optically transparent semiconductor is indium oxide. It has been extensively used in solar cells, liquid crystal displays, and microelectronic window heaters. Most of the studies involving indium-oxide nanoparticles or thin films have been focused on their electrical and optical properties. Various indium oxide nanostructures including nanoparticles, nanowires, and nanotubes have recently been synthesized using the vapor-liquid-solid method.[1,3] They possess remarkable qualities including strong electrical conductivity and great transparency to visible light.[4-6] In the treatment and management of cancerous and non-cancerous disorders, photodynamic therapy (PDT), a noninvasive method, is recognized for its low toxicity.[7-9] It includes the direct (topical) or systemic injection of a photosensitizer (PS) medicine, which when in contact with the right wavelength of light releases reactive singlet oxygen ($^1O_2$) species (visible or NIR). The effects of PDT are caused by this cytotoxic singlet oxygen. The PDT action stays isolated to the irradiated (diseased) spot because singlet oxygen has a short half-life and a small diffusion range in aqueous media (0.1µm), protecting nearby healthy tissues and cells from harm.[10-12] Although theoretically simple, the PDT method has many shortcomings. One disadvantage of PS medicines is their hydrophobic nature, which prevents optimal biodistribution and pharmacokinetics.[13-16] Incorporation of PS within aqueous dispersed nanoparticles can render aqueous formulations of PS. In the past decade, several reports involving nanoparticulate formulations of PS have surfaced, most of which involve porous and optically-transparent inorganic-based nanoparticles.[17-20] It may be noted that the release of the PS from the nano formulation is not a prerequisite for PDT action, as long as the nanoparticle matrix is permeable to the oxygen species.[21] We synthesized indium oxide nanoparticles and combined them with a PS molecule to see whether this may improve the PS's efficiency at producing singlet oxygen through photogeneration. Here, 2-diazo-3-oxo-5,10,15,20-tetraphenyl chlorin is the PS

molecule.[22] The synthesis of the blank and PS-incorporated nanoparticle system was carried out in methanolic media, with the surface stabilized by phenyl trisilanol. The nanoparticles were put into an aqueous solution after being synthesized. Then, they were examined using TEM, FTIR, UV-visible spectrophotometry, and spectrofluorimetric to describe them for different physical characteristics. The efficacy of photogeneration of singlet oxygen was compared for the free and nano-incorporated PS molecule. Finally, *in vitro* studies were performed to analyze the cellular uptake as well as light-induced cytotoxic effects of the PS-incorporated nanoparticles.

EXPERIMENTAL

Synthesis of the PS Molecule

Indium (III) nitrate hydrate (In $(NO_3)_3$.x H_2O), ammonium hydroxide, THF (tetrahydrofuran), sodium hydroxide, and methanol were procured from SRL (India). TritonX-100, Tris-HCl buffer, and 9, 10-ABMDMA (anthracenediyl-bis (methylene) dimalonic acid) were obtained from Sigma-Aldrich (United States). Amphotericin B, DMEM, FBS, antibiotics (streptomycin and penicillin), MTT Reagent (3-(4,5-dimethylthiazol-2-yl)-2,5-diphenyltetrazolium bromide), and other cell culture materials were procured from Genetix (India). ATCC (United States) provided human lung cancer A-549 cells.

Synthesis of Blank or PS-incorporated Indium Oxide Nanoparticles

The compound phenyl trisilanol $[(c\text{-}C_5H_9)_7Si_7O_9(OH)_3]$ was made using the earlier described technique.[23] A methanolic solution of the synthesized trisilanol in 45ml received sodium hydroxide (the ratio between sodium hydroxide and trisilanol was 3:1 in the feed molar). Then, at 30°C in an atmosphere of N_2, 1.5ml of each of the aqueous reactant solutions of {0.05 M of NH_4OH and 0.05 M $In(NO_3)_3$}, and 80µl of double-distilled water were poured to the sodium trisilanolate solution that had formed in the methanol. Instead of 80µl of water, the solution for the synthesis of PS-incorporated nanoparticles included an equivalent amount of PS/DMSO (2.4µM). For the nanoparticle synthesis process to be completed, the solution was left to agitate overnight. The resultant nanoparticles, either empty or containing PS, were then spun at 10,000 rpm for five minutes and cleaned thrice with pure methanol. The precipitate was then dried for a day at 50°C in a vacuum oven. The precipitate was suspended in THF by vigorous stirring, and the nanoparticles were then isolated by centrifugation (10,000rpm, 5min). The dried nanoparticles have been then dissolved in water for additional testing.

Characterization Studies

TEM was used to measure the size of the PS-incorporated nanoparticles. Onto formvar-coated 200 mesh copper grids (Ted Pella, United States), aqueous nanoparticle dispersion was sonicated, drop-coated, and dried. Imaging was then performed using a TECNAI G2-30 U TWIN TEM apparatus (FEI, Eindhoven, the Netherlands), with an accelerating voltage of 300V. Using a quasi-elastic light scattering device, DLS (dynamic light scattering) was used to further examine the size of the PS-incorporated nanoparticles distributed in distilled water (QELS, photocor-FC, Model-1135 P). The light source was a 633nm wavelength Helium-Neon laser. These measurements were done on a scattering angle of 90^0. The Perkin Elmer RX1 instrument was utilized to record the nanoparticles' FTIR spectra. With the help of a Cary Eclipse Fluorescence spectrometer (Varian, Palo Alto, CA), a UV-1601 spectrophotometer (Shimadzu, Kyoto, Japan), and, in some cases, nanoparticles with and without PS incorporated, the optical characteristics (fluorescence emission spectra and UV-visible absorption), were recorded for the nanoparticles. The PS-incorporation capacity of nanoparticles was also recorded using the same instrument as used above (Shimadzu UV-1601 spectrophotometer). After centrifugation, the free PS was separated from the nanoparticle-incorporated PS (10,000rpm, 5min). Following centrifugation, the supernatant's absorption spectra were captured. The PS amount in supernatant [S] was estimated spectrophotometrically by calculating the OD (optical density) at λ_{max} (430 nm). The incorporation efficiency was then calculated from the PS originally added [O].

$$E\% = [PS]_S / [PS]_O \times 100$$

Singlet Oxygen Detection by Photosensitizer *via* Photobleaching of ABMDMA

The chemical probe 9,10-anthracenediyl-bis(methylene) dimalonic acid was photobleached to measure photo-induced singlet oxygen generation (ABMDMA). A water-soluble anthracene derivative known as

ABMDMA may be photobleached by singlet oxygen to produce its equivalent endoperoxide. By measuring the drop in optical density at 400nm (the absorption λ_{max} of ABMDMA), the reaction is seen spectrophotometrically. In a typical experiment, PS-incorporated nanoparticles were combined with 15µM of the sodium salt of ABMDMA in water to achieve a final concentration of 0.24µM for PS. Two control sets included equivalent amounts of (a) ABMDMA and free PS, and (b) ABMDMA and blank nanoparticles. The solutions were continuously irradiated in an open quartz cuvette using a 630 nm diode laser (5mW), and every 15 minutes, the spectrophotometer measured their optical densities at 400nm.

***In vitro* Studies**

The DMEM medium in which the human lung cancer cell line A-549 was cultured was added with 1% streptomycin/penicillin, 10% FBS, and 1% amphotericin B. Using conventional cell growth techniques and the manufacturer's recommendations, the cells have been kept at 37°C and 5 percent CO_2 in a humidified incubator. The relative cellular absorption of PS in both its free and nano-incorporated forms was seen using fluorescence estimates from cell lysates. The cells were placed back in the incubator after being planted in 6-well plates that had been sterilized the day before the treatment with 200,000 cells and 2ml of a new medium in each well. The next day, aqueous dispersion of free PS and PS-incorporated nanoparticles (final PS concentration 0.24µM in both instances) was introduced to the cells at a confluency of about 70%, swirled, and then placed back in the incubator. The plate was removed from the incubator after 2h, the treatment medium was aspirated, and cells in the well were given two sterile PBS washes. After the cells had been thoroughly cleaned, they were lysed by adding 200µl of water containing 1 percent Triton X-100 to each well and incubating for 30 min with moderate shaking. The cells in the lysis solution were then scraped, combined with an extra 1ml of PBS/well, and put into microcentrifuge tubes. Centrifugation was then used to remove the cell debris from the lysate (3,000rpm, 5min). For examination of PS-related fluorescence in the spectrofluorometer, the supernatant (lysate) was obtained. For studying cell viability after PDT, 75,000 cells were plated in each well of two 24-well plates and incubated overnight for attachment and growth. The wells were cleaned carefully with sterile PBS 3 times the following day, and 500µl of fresh medium was added to each well. Next, triplicates of each of the following samples were given to each well: (a) free PS (0.24µM), (b) blank nanoparticles (100µg/ml), and (c) PS (.24µM)-incorporated nanoparticles (100µg/ml). After that, the two plates were put back in the incubator for 24h. Following three sterile PBS rinses, 500µL of the new medium was added to each well on both plates. Instantaneously, one of the plates was put back in the incubator (without light irradiation). The second plate was initially placed in the incubator before being treated to a 633nm laser light for 10 minutes in each well utilizing a diode laser with an output power of 5mW. The two plates were removed from the incubator after being incubated, and the MTT technique was used to determine their viability.[24] Triplicates of the experiment were performed. For estimating *in-vitro* cell viability *via* simple microscopic analysis after PDT treatment, cells plated in a 6-well format were treated with blank nanoparticles, free PS, and PS-incorporated nanoparticles. The wells were cleaned with sterile PBS after 24h of incubation, 1ml of the new medium was added to each well, and they were then immediately subjected to a 633nm laser light for 10 minutes each. Cells treated with the above samples but receiving no light irradiation served as controls. The plates have been put into the incubator again for the night. Following that, sterile PBS was used to rinse the wells, and 1 ml of fresh media was added to each well. The cells were subsequently examined under a microscope utilizing the phase-contrast images (ZEISS Axiovert 40 CFL).

RESULTS AND DISCUSSION

In Figs.-1(A) and (B), correspondingly, the TEM and DLS data of the produced PS-incorporated nanoparticles are displayed. TEM image depicted irregularly shaped particles with a diameter in the range of 30 to 50 nm. DLS plot shows the average hydrodynamic size of the aqueous dispersed nanoparticles to be 90 nm.

The FTIR spectra of standard indium oxide nanoparticles, Phenyl trisilanol, and synthesized indium oxide nanoparticles (IN-NPs) are shown in Fig.-2(A) shows the Standard spectra of indium oxide nanoparticles, the absorption peaks at 1640 cm^{-1} and 3400 cm^{-1} are attributable to the absorptions of hydroxyls from absorbed water, whereas the absorption band about 600 cm^{-1} is caused by Indium-oxygen bonds.[25]

Trisilanol spectrum (B) exhibits Si-O framework signals at (1100 cm^{-1} band), phenyl group peaks at 698 as well as 746 cm^{-1}, and Si-phenyl interaction signals at 1150 cm^{-1} and 1462 cm^{-1}.[26] Particularly, signals related to C-H on phenyl group peak occur in the 3000-3100 cm^{-1} range.[27-28] Spectrum C shows the absorption band 600 cm^{-1} formed by metal-oxygen bonds (In-oxygen), while the other peaks are similar to that of spectra B because of the same material used for the synthesis of indium oxide nanoparticles.

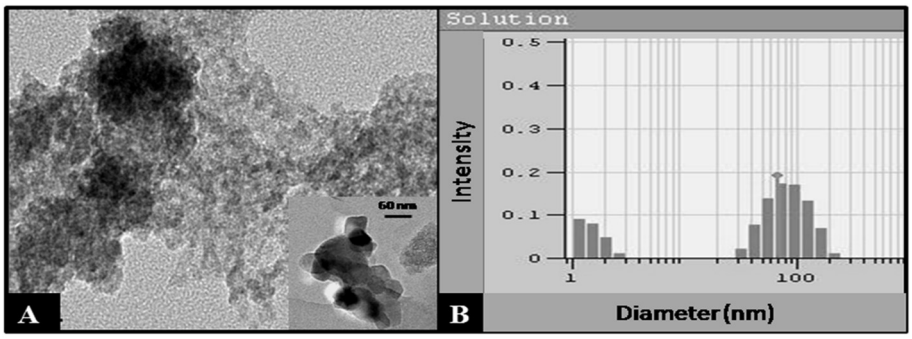

Fig.-1: (A) TEM Image, (B) DLS Plot, (C) Powder XRD Spectrum of Indium Oxide (IN) Nanoparticles

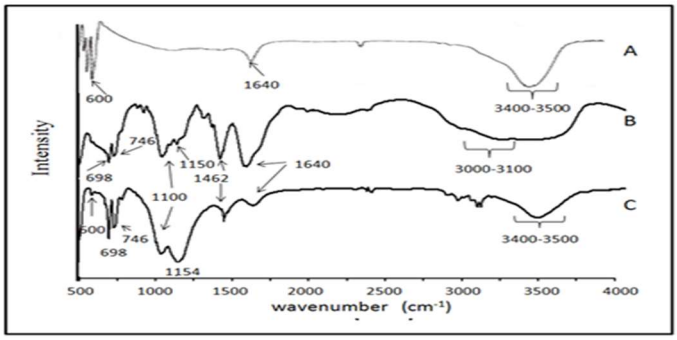

Fig.-2: FTIR Spectra of (A) Standard Indium Oxide Nanoparticles (B) Trisilanol (C) IN NPs, (D) Chitosan (CH) (E) IN-NPs Coated with Chitosan (IN-CH)

Next, we investigated the functional effects of PS incorporation within these nanoparticles. The chemical structure and absorption spectrum of the PS are illustrated in Fig.-3(A) and (B), correspondingly.

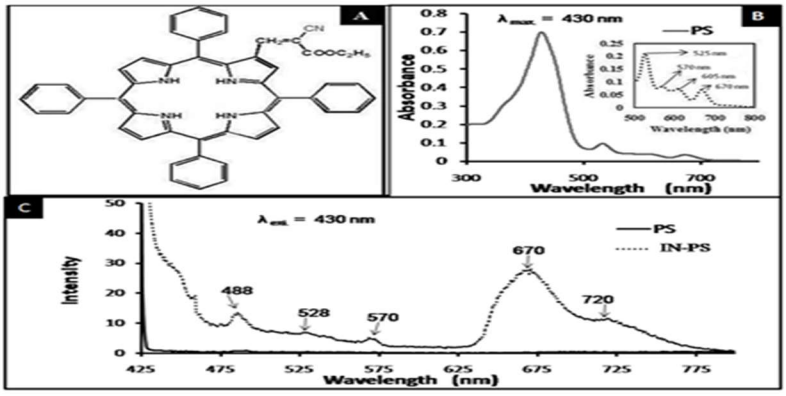

Fig.-3: (A) Shows the Structure of the PS (B). The Absorbance Spectra of PS in DMSO Solution (C) Emission Spectra of an Aqueous Dispersion of Free PS (Photosensitizer) and PS-IN (Indium Oxide-Photosensitizer)

The absorption spectrum of the PS shows a primary absorption peak at 430 nm, and several secondary absorption peaks (Q-bands) appearing at 525, 570, 605, and 670 nm. Figure-3 (C) shows the fluorescence emission spectra (λ_{ex} = 430 nm) of aqueous dispersions of free PS and PS-incorporated nanoparticles. Fluorescence spectra show that when photosensitizer is incorporated with the nanoparticles, we obtained various characteristic emission peaks of the PS (488, 528, 570, 670, and 720 nm), while there is no peak

in the case of free PS. This is because while the water-insoluble PS is in an aggregated state in its free form (with ensuing concentration quenching), the nano-incorporated PS remains non-aggregated in its microenvironment.

Utilizing the chemical approach of 9, 10-anthracenediyl-bis(methylene) dimalonic acid, we were able to demonstrate singlet oxygen synthesis (ABMDMA). Figures-4(A), 4(B), and 4(C) show the decrease in optical density (OD) at 400nm (absorption λ_{max} for ABMDMA) as a laser exposure time function, for free PS, blank nanoparticles, and PS-incorporated nanoparticles, respectively. Figure-4(D) shows the summary data for all these three graphs. The plots for PS-incorporated nanoparticles show an appreciable decrease in OD (corresponding to the singlet oxygen-mediated photobleaching of ABMDMA) with the light exposure time, revealing the efficient singlet oxygen generation. There was no observable difference in the OD of ABMDMA with the exposure time for free PS and blank nanoparticles.

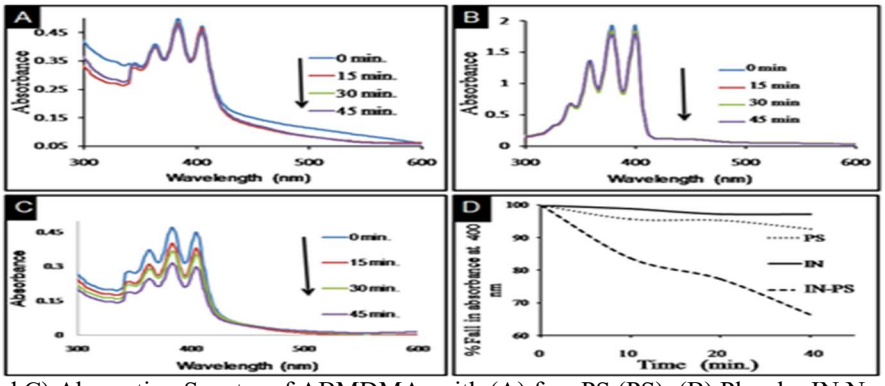

Fig.-4: (A, B, and C) Absorption Spectra of ABMDMA, with (A) free PS (PS), (B) Placebo IN Nanoparticles (IN), and (C) PS-Encapsulated IN Nanoparticles (PS-IN), Following Laser Irradiation for A Specific Time (in mins). (D) Results From All Three Systems Combined Demonstrated a Reduction in OD at 400nm (ABMDMA Absorption Maxima) as a Function of Laser Irradiation Duration

This experiment indicated that the singlet oxygen photogeneration from the photosensitizer is possible when incorporated within the nanoparticles, which provides it with non-aggregated aqueous dispersion. Analysis of cell uptake was utilized to compare the absorption of nano-incorporated and free PS. Figure-5(A) demonstrates that the PS has increased cellular uptake when it is incorporated within the nanoparticles, as determined by measuring the PS-associated emission from the lysates of treated cells. We next probed the photoactivated toxicity of cells (*in vitro* PDT) treated with PS, in both free and nano-incorporated forms. The phototoxicity data is represented in Fig.-5(B). This information demonstrates that even after light irradiation, the cells treated with free PS and blank nanoparticles maintained more than 90% of their viability. In contrast, cells treated with PS-incorporated nanoparticles showed a significant amount of cell death (approximately 50% cell viability); whereas the same cells without light irradiation remained about 80% viable. This is a demonstration of *in vitro* PDT using PS-incorporated nanoparticles. It is worth mentioning that we are using very low laser light power (about 5 mW) in our experiments. Nevertheless, the PDT efficacy is very encouraging.

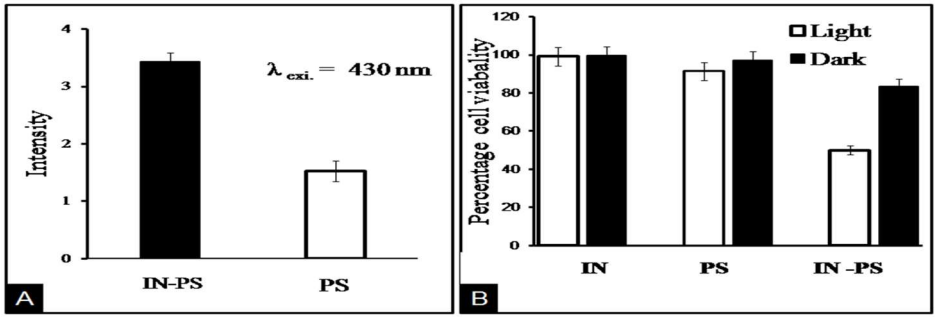

Fig.-5: (A) Quantitative Measurement of Fluorescence Retrieved from Cell Lysates after PS-IN and PS Treatment (B) Percentage of A-549 Cells that Survived after Being Treated with Different Solutions and after being Exposed To 633nm Laser Light Both in the Light and in the Dark

We have performed a similar *in vitro* PDT experiment, where the cell viability was monitored by observing the morphology of treated cells using a phase-contrast microscope. As in the previous experiment, the cells underwent treatments with blank nanoparticles, free PS, and PS-incorporated nanoparticles, without and with light irradiation. It can be seen from Fig.-6 that only in the cells receiving treatment with PS-incorporated nanoparticles and subsequent light irradiation do we see distorted morphology akin to dying cells. All the other cells looked morphologically healthy.

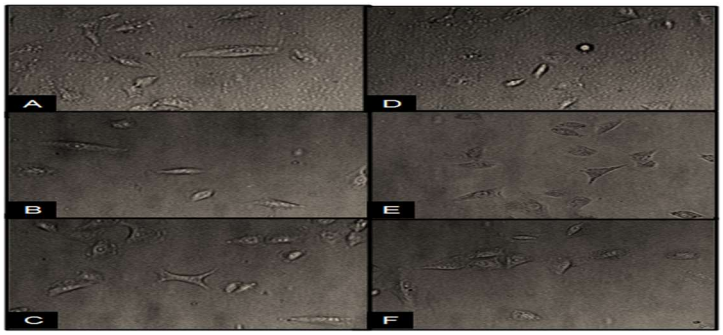

Fig.-6: Microscopic Phase Contrast Images of A-549 Cells Treated with (A, D) PS-IN Nanoparticles, (B, E) Free Photosensitizer (PS), and (C, F) Placebo IN Nanoparticles. (A, B, C) without Light Irradiation; and (D, E, F) with Light Irradiation

This data confirms that only a combination of nano-incorporated PS and light exposure causes cytotoxicity. Blank nanoparticles and free PS are largely non-toxic, even after light exposure. Thus, PS-incorporated indium oxide nanoparticles appear to be promising drug carriers in PDT.

CONCLUSION

To sum up, it seems that these nanoparticles are capable of incorporating lipophilic PS and providing a stable aqueous dispersion for the PS. Trisilanol ligands were used to modulate nanoparticle growth during synthesis, leading to a uniform distribution in an aqueous solution. Experiments with the synthesis of singlet oxygen revealed that this oxygen is responsible for the bleaching of ABMDMA after laser light irradiation of PS-incorporated nanoparticles, but not of free PS.

REFERENCES

1. A. Murali, A.B. Valerie, J. Leppert, and R H Subhash, *Nano Letter*, **1**, 287(2001)
2. S. Pissadakis, S. Mallis, L. Reekie, S.J. Wilkinson, W.R. Eason, Vainos N A, K. Moschovis and G. Kiriakidi, *Applied Physics,***169**, 333(I999)
3. G.B. Lewis and C.D. Paine, *Materials Research Bulletin*, **25**, 22(2000)
4. A. Henglein, *Chemical Reviews,* **89**,1861(1989), https://doi.org/10.1021/cr00098a010
5. P.A. Alivisatos, *Journal of Physical Chemistry,* **100**, 13226(1996), https://doi.org/10.1021/jp9535506
6. C. Burda, X. Chen, R. Narayanan and M.A. El-Sayed, *Chemical Reviews,* **105**,1025(2005), https://doi.org/10.1021/cr030063a
7. M. Triesscheijn, P.Baas, S M.H.J. Chellens and A.F. Stewart, *Oncologist*, **11**,1034(2006), https://doi.org/10.1634/theoncologist.11-9-1034
8. G.Y. Qiang, P.X. Zhang, J. Huang, and Z. Li, *Chinese Medical Journal,**119***,845 (2006) https://doi.org/10.1097/00029330-200605020-00009
9. G.P. Calzavara-Pinton, M. Venturini and R. Sala, *Journal of Photochemistry and Photobiology B: Biology,***78,**1(2005), https://doi.org/10.1016/j.jphotobiol.2004.06.006
10. J.G.J.E.D. Dolmans, D. Fukumur, and K.R. Jain, *Nature Reviews Cancer,* **3**, 380(2003), https://doi.org/10.1038/nrc1071
11. J.I. MacDonald and J.T. Dougherty, *Phthalocyanines,* **5**,105(2001)
12. N.L. Oleinick, R.L. Morris and I. Belichenko, *Photochemical and Photobiological Sciences,* **1**,1(2002)
13. M. Kastle, S. Grimm, R. Nagel, N. Breusing and T. Grune, *Biology and Medicine,* **50**, 305(2011)

14. G. Charron, T. Stuchinskaya, R. Edwards, A.D. Russell and T. Nann, *The Journal of Physical Chemistry C,* **116**, 9334(2012), https://doi.org/10.1021/jp301103f
15. K. Hirakawa, T. Hirano, Y. Nishimura, T. Arai and Y.Nosaka , *The Journal of Physical Chemistry B*, **116**, 3037(2012), https://doi.org/10.1021/jp300142e
16. Y. Cheng, D.J Meyers, M.A. Broome, E.M. Kenney, P.J. Basilion, and J.C. Burda, *American Chemical Society,* **133**, 2583(2011)
17. I. Roy, Y.T Ohulchanskyy, E.H. Pudavar, J.E. Bergey, R.A. Oseroff, J. Morgan, T. J. Dougherty and N.P. Prasad, *Journal of the American Chemical Society*,**125,**7860(2003), https://doi.org/10.1021/ja0343095
18. L. Zhou, C. Dong C, H.S. Wei, Y.Y. Feng, H.J. Zhou and H.J. Liu, *Material Lett*ers, **63**, 1683(2009), https://doi.org/10.1016/j.matlet.2009.05.010
19. L. Zhou, H.J. Liu, F. Ma, H.S. We, Y.Y. Feng, H.J. Zhou, Y.B. Yu, and J. Shen, *Journal of Biomedical Microdevices,* **12**, 655(2010)
20. L. Zhou, J.H. Liu, J. Zhan, H.S. Wei, Y.Y. Feng, H.J. Zhou, Y.B. Yu, J. Shen, *International Journal of Pharmaceutics*, **386**,131(2010)
21. T. Hasan, Photodynamic Therapy: Basic Principles and Clinical Applications Mercel Dekker New York, (1992)
22. T. Köpke, M. Pink, J.M. Zaleski, *Synlett,* **14**, 2183(2006)
23. F. J. Feher, T. A. Budzichowski, R. L. Blanski, K. J. Weller and J. W. Ziller, *Organometallics*, **10**, 7(1991)
24. I. Roy, Y.T Ohulchanskyy, E.H. Pudavar, J.E. Bergey, R.A. Oseroff, J.Morgan, T. J. Dougherty and N.P. Prasad, *Journal of the American Chemical Society*,**125**,7860(2003), https://doi.org/10.1021/ja0343095
25. C. Chen, D. Chen, X. Jiao and C. Wang, *Chemical Communication*, **44** ,4632(2006)
26. D. Lin-Vien, B.N. Colthup, G.W. Fateley and G.J Grasselli, *The Handbook of Infrared and Raman Characteristics Frequency of Organic Molecules Academic Press Inc. San Diego CA,* (1991)
27. C.P. Eklund, M.J. Golden, A.R. Jishi, *Carbon*, **33**, 959(1995), https://doi.org/10.1016/0008-6223(95)00035-C
28. A. Galvez, N. Herlin-Boime, C. Reynaud, C. Clinard, and N.J. Rouzaud, *Carbon,* **40**, 2775(2002)

[RJC-6289/2021]